Author(s): Lehtinen, Noora; Suhonen, Janne; Rice, Kiesha; Välimäki, Eetu; Toriseva, Mervi; Routila, Johannes; Halme, Perttu; Rahi, Melissa; Irjala, Heikki; Leivo, Ilmo; Kallajoki, Markku; Nees, Matthias; Kuopio, Teijo; Ventelä, Sami; Rantala, Juha K.

Title: Assessment of targeted therapy opportunities in sinonasal cancers using patient-derived functional tumor models

Year: 2024

Version: Published version

Please cite the original version:

Lehtinen, N., Suhonen, J., Rice, K., Välimäki, E., Toriseva, M., Routila, J., Halme, P., Rahi, M., Irjala, H., Leivo, I., Kallajoki, M., Nees, M., Kuopio, T., Ventelä, S., & Rantala, J. K. (2024). Assessment of targeted therapy opportunities in sinonasal cancers using patient-derived functional tumor models. Translational Oncology, 44, Article 101935. https://doi.org/10.1016/j.tranon.2024.101935

Translational Oncology 44 (2024) 101935

Contents lists available at ScienceDirect

Translational Oncology

journal homepage: www.elsevier.com/locate/tranon

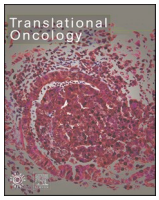

Original Research

Assessment of targeted therapy opportunities in sinonasal cancers using patient-derived functional tumor models

Noora Lehtinen [a], Janne Suhonen [a], Kiesha Rice [a], Eetu Välimäki [a], Mervi Toriseva [b,c], Johannes Routila [b,d], Perttu Halme [b,d], Melissa Rahi [e,f], Heikki Irjala [b,d], Ilmo Leivo [b,g], Markku Kallajoki [g], Matthias Nees [b,c,h], Teijo Kuopio [i,j], Sami Ventelä [b,c,d,#], Juha K. Rantala [a,#,*]

[a] *Misvik Biology Oy, Turku, Finland*
[b] *Turku Bioscience Centre, University of Turku and Åbo Akademi University, Turku, Finland*
[c] *FICAN West Cancer Centre, Turku, Finland*
[d] *Department for Otorhinolaryngology - Head and Neck Surgery, University of Turku and Turku University Hospital, Turku, Finland*
[e] *Department of Neurosurgery, Neurocenter, Turku University Hospital, Turku, Finland*
[f] *Clinical Neurosciences, University of Turku, Turku, Finland*
[g] *Department of Pathology, University of Turku and Turku University Hospital, Turku, Finland*
[h] *Department of Biochemistry and Molecular Biology, Medical University of Lublin, Lublin, Poland*
[i] *Department of Biological and Environmental Science, University of Jyväskylä, Jyväskylä, Finland*
[j] *Wellbeing Services County of Central Finland, Jyväskylä, Finland*

ARTICLE INFO

Keywords:
Sinonasal cancer
Ex vivo drug screening
Driver mutation
Targeted therapy

ABSTRACT

Malignant tumors derived from the epithelium lining the nasal cavity region are termed sinonasal cancers, a highly heterogeneous group of rare tumors accounting for 3 – 5 % of all head and neck cancers. Progress with next-generation molecular profiling has improved our understanding of the complexity of sinonasal cancers and resulted in the identification of an increasing number of distinct tumor entities. Despite these significant developments, the treatment of sinonasal cancers has hardly evolved since the 1980s, and an advanced sinonasal cancer presents a poor prognosis as targeted therapies are usually not available. To gain insights into potential targeted therapeutic opportunities, we performed a multiomics profiling of patient-derived functional tumor models to identify molecular characteristics associated with pharmacological responses in the different subtypes of sinonasal cancer.

Methods: Patient-derived *ex vivo* tumor models representing four distinct sinonasal cancer subtypes: sinonasal intestinal-type adenocarcinoma, sinonasal neuroendocrine carcinoma, sinonasal undifferentiated carcinoma and SMARCB1 deficient sinonasal carcinoma were included in the analyses. Results of functional drug screens of 160 anti-cancer therapies were integrated with gene panel sequencing and histological analyses of the tumor tissues and the *ex vivo* cell cultures to establish associations between drug sensitivity and molecular characteristics including driver mutations.

Results: The different sinonasal cancer subtypes display considerable differential drug sensitivity. Underlying the drug sensitivity profiles, each subtype was associated with unique molecular features. The therapeutic vulnerabilities correlating with specific genomic background were extended and validated with *in silico* analyses of cancer cell lines representing different human cancers and with reported case studies of sinonasal cancers treated with targeted therapies.

Abbreviations: BSA, bovine serum albumin; CCLE, Cancer Cell Line Encyclopedia; CK, cytokeratin; GR, growth rate; HDAC, histone deacetylase; IHC, immunohistochemical; ITAC, intestinal-type adenocarcinoma; MSI, microsatellite instability; NGS, next-generation sequencing; RT, room temperature; SDSC, SMARCB1 deficient sinonasal carcinoma; SNC, sinonasal cancer; SNEC, sinonasal neuroendocrine carcinoma; SNSCC, squamous cell carcinoma; SNUC, sinonasal undifferentiated carcinoma.

* Corresponding author at: Misvik Biology Oy, Karjakatu 35 B, FI 20520, Turku, Finland.
E-mail address: rantala@misvik.com (J.K. Rantala).
# Equal contribution.

https://doi.org/10.1016/j.tranon.2024.101935
Received 13 December 2023; Received in revised form 26 February 2024; Accepted 7 March 2024
Available online 23 March 2024

Conclusion: The results demonstrate the importance of understanding the differential biology and the molecular features associated with the different subtypes of sinonasal cancers. Patient-derived *ex vivo* tumor models can be a powerful tool for investigating these rare cancers and prioritizing targeted therapeutic strategies for future clinical development and personalized medicine.

Introduction

The inner lining of the nasal cavity and paranasal sinuses is a highly specialized epithelial tissue. The tissue architecture of the epithelium in the anterior nasal cavity is similar to external skin containing keratinized stratified squamous epithelium with hair follicles, sweat glands, and sebaceous glands. The epithelium lining the posterior nasal vestibule is a non-keratinized, stratified squamous epithelium that transitions into pseudostratified columnar epithelium lining the inner nasal cavity and paranasal sinuses. Tumors originating from the sinonasal tract comprise a highly heterogeneous group of histological subtypes [1–4], including squamous cell carcinoma (SNSCC), intestinal-type adenocarcinoma (ITAC), non-intestinal-type adenocarcinoma, SWI/SNF complex deficient sinonasal carcinoma with five subtypes including the SMARCB1 (INI-1) deficient sinonasal carcinoma (SDSC), olfactory neuroblastoma, sinonasal neuroendocrine carcinoma (SNEC), sinonasal undifferentiated carcinoma (SNUC), and sinonasal melanoma. In addition to this main histopathological classification, many subtypes may have various histological growth patterns e.g. papillary, colonic, solid, mucinous and others [5]. Due to the overall low incidence rate (0.83 per 100,000 individuals) of sinonasal cancers (SNCs) [6], and the high number of different subtypes, the development of novel treatments for the different SNCs is challenging. Surgical resection remains the treatment of choice across all subtypes of SNC. If adjuvant therapy is needed, a chemoradiotherapy strategy dating back to the early 1980s with cisplatin, docetaxel, or 5-FU is considered [6]. To date, no SNC-specific clinical studies of targeted therapies have been reported and the prognosis of SNCs, particularly in advanced diseases, is poor (45.7 % 5-year survival [7]). Therefore, there is an imminent need for alternative treatment strategies for neoadjuvant therapy in SNC.

The past decade has yielded significant increases in biological knowledge and understanding of the genetic and molecular features associated with the different subtypes of SNCs. Next-generation sequencing (NGS) data from individual studies profiling small cohorts of sinonasal tumors also suggest opportunities for targeted therapies in a substantial proportion of patients based on actionable genetic alterations. These include e.g., EGFR/HER2-TKI in SNSCCs without activating RAS/RAF mutations [8,9], IDH inhibitors in SNUC and SNEC [10] and immune oncology treatments including immune checkpoint inhibitors across various SNCs based on microsatellite instability (MSI) status [11] and PD-L1 expression [12,13]. Systematic clinical development of these treatments is, however, complicated by the low number of patients, e.g., in average only 54.8 cases diagnosed annually in Finland (5-year average, 2017–21). In addition, the lack of established pre-clinical models limit the ability to perform detailed *in vitro* studies on specific subtypes of SNCs.

To gain insights into the general drug responsiveness of different subtypes of SNCs, we sought to use patient-derived functional tumor models to study drug efficacy in different SNC subtypes. Vital tumor cells isolated directly from surgical tissue samples of ITAC, SNEC, SNUC, and SDSC tumors were utilized for comparative *ex vivo* drug screening with a comprehensive drug library of 160 anti-cancer agents. The resulting differential drug sensitivity profiles were then correlated with oncogene targeted genetic profiling and immunohistology analyses of the tumors. The results highlight considerable differences in sensitivity to various targeted cancer drugs across the different SNC subtypes consistent with results obtained in various human cancers with shared driver aberrations. The results thus support recent data suggesting that each SNC subtype is associated with different, yet potentially targetable genomic aberrations.

Materials and methods

SNC patient samples

The use of SNC patient samples for research was approved by the Finnish National Supervisory Authority for Welfare and Health (V/39,706/2019) and the regional ethics committee of the University of Turku (51/1803/2017 and 166/1801/2015). The study was conducted according to the guidelines of the Declaration of Helsinki. Altogether, four patients were diagnosed with a SNC over a one-year period in our center and all were included to this study. These cases represented ITAC, SNUC, SNEC, and SDSC subtype. The patients were identified after confirming the biopsies taken from the tumor of the nasal cavity and analyses performed by pathologist. Thereafter, the selected patients were invited to participate and sign a written informed consent by a head and neck surgeon at the Turku University Hospital. The tissue samples of each SNC subtype were collected during surgery and placed into a sterile RPMI-1640 medium (Gibco) to be delivered to the research laboratory for *ex vivo* drug screening and molecular characterization. Following standard procedures, the rest of the tumor tissue was fixed in 4 % buffered formaldehyde and embedded in paraffin wax at the Pathology department following standard procedures. Tissue sections were stained with hematoxylin and eosin, and the pathologist evaluated the quality of the samples. All immunohistochemical (IHC) stains (Table S1.) were performed according to routine clinical diagnostic protocols and examined by pathologists for diagnosis. The tumor tissue was processed immediately in the research laboratory for *ex vivo* drug screening, as described [14]. Briefly, the tissues were cut into small pieces and digested enzymatically using pure collagenase (200 U/ml, Gibco, Life Technologies). The number of cells in the resulting cell suspension was counted with a Cellometer Mini cell counter (Nexcelom). A total of 7×10^5 cells was used for initial *ex vivo* drug screening immediately on the day of operation. The rest were used to attempt long term propagation in standard cell culture conditions (37 °C, 5 % CO2) in RPMI – 1640 medium supplemented with penicillin/streptomycin (100 units/100 mg), l-glutamine (2 mmol/L) and fetal bovine serum (1 %, Biowest). The medium of cell cultures was changed twice a week, and confluent cultures were dissociated with TrypLE Select enzyme (Gibco) and split 1:2 into new cultures.

Ex vivo drug screening

Ex vivo drug screens were performed using a library of 160 therapeutic compounds consisting of approved anti-cancer agents including all standard of care treatments and investigational compounds selected to cover key signaling pathways and targets. All drugs were purchased from commercial chemical vendors (Selleck Biochemicals, Adooq, MedChemExpress). The experiments were performed in 384-well microplate format as previously described [15]. Briefly, each drug compound was tested in four different concentrations with 2-fold dilutions and a dose range adjusted separately for each drug. The cells isolated from the tumor tissues were dispensed as a single cell suspension into two 384-well plates readily containing the drugs. Cells were incubated with the drugs in standard cell culturing conditions (37 °C, 5 % CO_2) for 96 h.

Enzymatic cell viability assay

The drug responses were evaluated with an enzymatic cell viability assay as described [16]. Briefly, the assay was performed following a 96-h incubation of the cells in plates containing the drugs to define drug-induced growth inhibition. Cell viability was measured using CellTiter-Glo reagent (Promega) according to the manufacturer's instructions with a luminescence plate reader (Labrox, Turku, Finland).

DNA extraction and targeted deep sequencing

DNA was isolated from cultured early passage tumor cells ($\sim 5 \times 10^5$ cells) or microdissected, representative tumor sections from the FFPE tumor sample of SDSC evaluated by a pathologist at Turku University Hospital. NucleoSpin Tissue DNA purification kit (Macherey-Nagel GmbH) was used for DNA isolation according to the manufacturer's instructions. DNA was quantified using a Qubit fluorometer (Thermo Fisher Scientific). Targeted deep sequencing was performed using the hybridization-based target capture INVIEW Oncopanel All-in-one (version 2.8) (Eurofins Genomics, Konstanz, Germany) [17]. The panel covers the entire exons of 591 cancer-associated genes. The NGS data analysis was performed by Eurofins Genomics with a validated NGS analysis pipeline. Single nucleotide variants, insertions, and deletions (In/Del) were detected and filtered based on mutation allele frequency (>1 %) and variants were annotated for known clinical significance in a ClinVar (released 02. Oct 2017) database. The sequencing data files are deposited to EMBL-EBI European Nucleotide Archive (ENA) under accession no. ERP154225.

Immunohistochemistry

Routine IHC stains were performed at the Department of Pathology of Turku University Hospital as described [18] (list of the used immunohistochemical markers is provided in Table S1). For confocal microscopy, primary cell spheroids (ITAC) were fixed with 4 % paraformaldehyde for one h at room temperature (RT), permeabilized with 0.5 % Triton-X100 for 15 min at RT and stained with immunocytochemistry. Briefly, the spheroids were blocked with 3 % bovine serum albumin (BSA) in PBS (30 min, RT) and subsequently incubated in primary antibody suspension in rotation over night at 4 °C (each 1:100 in 3 % BSA-PBS). The primary antibodies used were anti-panCK (ab86734, mouse, Abcam) and anti-CDX2 (clone EPR2764Y, rabbit, Sigma-Aldrich). After washing, the spheroids were incubated with fluorescent secondary antibodies anti-mouse 647 (A31571, Life Technologies) and anti-rabbit 488 (A32731, Invitrogen), and with Alexa Fluor 546 phalloidin (A22283, Invitrogen) in rotation over night at 4 °C (each 1:200 in 3 % BSA-PBS). Hoechst 33,258 (1:2000) was used for DNA counterstaining. After washing, the spheroids were spun down and mounted under a coverslip for imaging. Confocal microscope images were acquired with 3i CSU-W1 spinning disk microscope, 40x Zeiss LD Plan-Neofluar objective, and Photometrics Prime BSI sCMOS camera, controlled with Slidebook 6 software.

Statistical analysis

Ex vivo drug screening data were analyzed using the normalized growth rate inhibition (GR) yielding per-division metrics for drug potency and efficacy as described [19]. IC50 value calculations and all other statistical analyses were performed with Prism 10 statistical software (GraphPad, v.10.0.3). *In silico* analyses of drug efficacy and gene expression in established cancer model cell lines were done using data obtained from the Cancer Cell Line Encyclopedia (CCLE) [20] .

Results

In this study, a vital tumor sample from four patients representing four different SNC subtypes was collected for comparative functional *ex vivo* analysis and molecular profiling (Fig. 1). Cells isolated immediately on the day of operation by enzymatic dissociation of the tumor tissues were used for high-throughput drug screens and targeted DNA NGS. A viability-based *ex vivo* drug sensitivity screen with 160 drugs was performed with each sample to gain insights into the different drug sensitivity of the different SNCs and to identify potential tumor and cancer type specific therapeutic vulnerabilities associated with the underlying genetic aberrations. To identify the most potent cytotoxic drugs with tumor-selective activity, we compared the growth rate corrected drug responses between the different SNCs representing functional tumor models (Figure S1). The results indicate that even though the sinonasal tumor subtypes are grouped broadly as SNCs for therapeutic purposes, they all represent biologically highly different forms of cancer with considerably different and unique genetic and molecular backgrounds (Table S1) and different biological characteristics, and that these variable features are reflected at the level of selective individual therapeutic sensitivities.

Drug sensitivity in sinonasal ITAC

ITAC is the second most frequent epithelial tumor of the sinonasal tract. Sinonasal ITACs are histologically highly reminiscent of intestinal adenocarcinoma and usually positive for "intestinal" IHC markers CK20, CDX2, MUC2, and villin, and variably positive for CEA [21–23], and they display a normal expression of DNA mismatch repair proteins, β-catenin, and E-cadherin [24]. Due to the close resemblance of colorectal adenocarcinoma and sinonasal ITAC, genetic studies have focused mainly on genes involved in pathogenesis of colorectal adenocarcinoma. These studies have shown that, unlike colorectal carcinomas, activating mutations in *KRAS* or *BRAF* genes and MSI are rare in sinonasal ITACs [8,9,11,25,26]. In a small subset of cases, somatic variants of *PIK3CA, APC, ATM, NF1, LRP1B,* and *BRCA1* genes have been identified [27], and only a low proportion of sinonasal ITACs have a *TP53* mutation [28–30]. The ITAC patient sample included in this study was obtained from a 69-year-old male who had tumor tissue in both nasal cavities (Fig. 2A). He had no history of exposure to carcinogenic factors such tobacco or occupational hardwood dust consistent with a sporadic case of ITAC. Radical surgical treatment was performed. Immunohistochemical analyses including the expression of CDX2 and CK20 were used to confirm the diagnosis of sinonasal adenocarcinoma of ITAC type (Fig. 2B). Cells isolated from the tumor tissue exhibited a peculiar characteristic of spontaneously forming spheroids (Figure S2A) with reversed polarity (Figure S2B) and functioning intestinal villi on the outer surface resulting in a continuous motility of the spheroids in culture (Video S1). The drug sensitivity profile of the cells in the *ex vivo* drug screen revealed significant and selective enrichment of drugs targeting EGFR/MAPK pathways in comparison to the other SNC samples (Fig. 2C). Included among the therapies exhibiting highest selective efficacy in the sinonasal ITAC were e.g., EGFR inhibitor cetuximab, B-Raf inhibitor dabrafenib, and MEK inhibitors trametinib and selumetinib (Fig. 2C). On the other hand, generally high potency drugs such as histone deacetylase (HDAC) inhibitors including vorinostat showed weaker efficacy on the sinonasal ITAC cells in comparison to the other SNCs (Fig. 2C). To assess potential driver aberrations associated with the increased sensitivity of the cells to EGFR/MAPK therapy (Fig. 2D), DNA sequencing of the sample cells was performed. Only intron variants of unknown significance in the genes involved in MAPK pathway were found including *BRAF, ERBB3, ERBB4* and *AKT1*. Based on the sensitivity of the cells to EGFR inhibition, IHC staining of EGFR was performed to assess protein level EGFR expression in tumor tissues. Results confirmed a strong membranous staining (intensity of 2+ on a scale of 1 to 3+) indicating EGFR overexpression (Fig. 2E). Since sinonasal ITAC and intestinal carcinomas both express *CDX2*, we investigated whether *CDX2* as a biomarker associate with responsiveness of cancer cells to drugs targeting EGFR/MAPK pathway. For this purpose, we compared

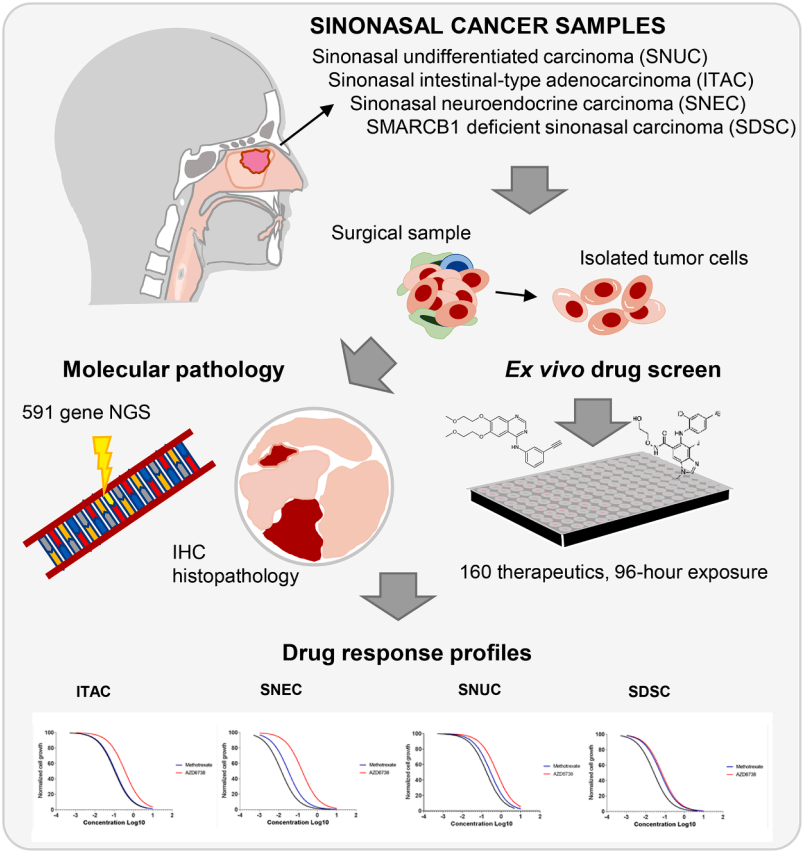

Fig. 1. Schematic presentation of the study design.

the efficacy (AUC) of 265 drugs between *CDX2* expressing and negative cell lines included in the CCLE (Fig. 2F). A total of 52 of 921 cell lines (with both RNA expression and drug response data available) were found to express *CDX2*. A total of 42 of these were of gastric or colorectal origin showing that *CDX2* is a highly specific and sensitive marker of intestinal differentiation [31]. Correlating with results from *ex vivo* drug screens in the sinonasal ITAC cells, the *CDX2* expressing cancer cell lines as a group were found to be significantly more sensitive to several EGFR and MEK inhibitors (Fig. 2F-H) and most resistant to HDAC inhibitors including entinostat (Fig. 2F). As MEK inhibitor sensitivity is generally associated with activating RAS mutations, we assessed next if the sensitivity of *CDX2* positive cell lines to MEK inhibition was dependent on *KRAS*-mutation status. No statistically significant difference in sensitivity between $KRAS^{mut}$ and $KRAS^{wt}$ -*CDX2* positive cell lines was observed suggesting that cellular differentiation state defined by *CDX2* expression could serve as an indicator of MAPK pathway dependency independent of *KRAS* mutation status (Figure S2C).

Drug sensitivity in SNEC

SNEC is a sinonasal tumor with neuroendocrine differentiation. It can be distinguished from other SNCs by immunohistochemical expression of common neuroendocrine markers such as neuron-specific enolase, synaptophysin, and chromogranin A (Table S1). Only a few publications on this tumor type are available, and no effective therapeutic options currently exist for SNEC. It is known that loss and inactivating mutations in *TP53* and *RB1* are widely observed in small-cell/neuroendocrine cancers of e.g., lung and prostate, and that neuroendocrine cancers across different tissues of origin resemble each other [32,33]. The SNEC sample included in the study was obtained from a 68-year-old female patient with a large sinonasal tumor in the anterior nasal cavity and the left ethmoidal cavity, with axial cross-sectional dimensions of about 3.4 × 2.4 cm, and tumor protruding in the left medial corner of the orbit (Fig. 3A). In the histopathological examination, the tumor was diagnosed as a poorly differentiated neuroendocrine carcinoma based on its positivity for the IHC markers chromogranin and synaptophysin (Fig. 3B). Extensive surgical treatment was performed, including evacuation of the contents of the left orbit. An *ex vivo* sample was obtained from the surgical resection. The drug screen indicated the SNEC cells displayed limited responsiveness to targeted therapies such as the EGFR/MAPK targeting drugs. Compared to the other SNC samples, SNEC cells were significantly more sensitive to general cytotoxic drugs inhibiting e.g., DNA replication, cell division, and epigenetic mechanisms (Fig. 3C). Among drugs showing highest selective efficacy in the SNEC cells were cyclin-dependent kinase inhibitor palbociclib, tubulin modulator vincristine, topoisomerase inhibitor epirubicin, DNA replication inhibitor hydroxyurea, and HDAC inhibitors belinostat and vorinostat (Fig. 3C). NGS profiling identified a limited number of known mutations associated with small cell/neuroendocrine tumors. *TP53* (p.L383fs), *SUFU* (p.A340S) and *EZH2* (p.L50S) mutations were the only identified aberrations with a potential neuroendocrine predisposing/associating function [34,35]. Also, point mutations of unknown significance in *CCND3* gene and intron variants in *RB1* gene were identified. To validate the differential drug sensitivity pattern of the SNEC cells in comparison to other cancers, we divided the cell lines in CCLE into neuroendocrine and non-neuroendocrine groups based on chromogranin A expression and compared the efficacy of 265 drugs between the groups (Fig. 3D). The drug sensitivity/resistance profile of the cell lines with neuroendocrine properties supported the observations from the drug screen with SNEC cells. The neuroendocrine differentiated cell lines as a group exhibited significantly increased resistance to targeted therapies including EGFR/RAS/MAPK pathway targeting drugs (Fig. 3D). Of these drugs, the EGFR-TKI gefitinib and in particular the MEK inhibitor selumetinib, had a significantly weaker effect on all

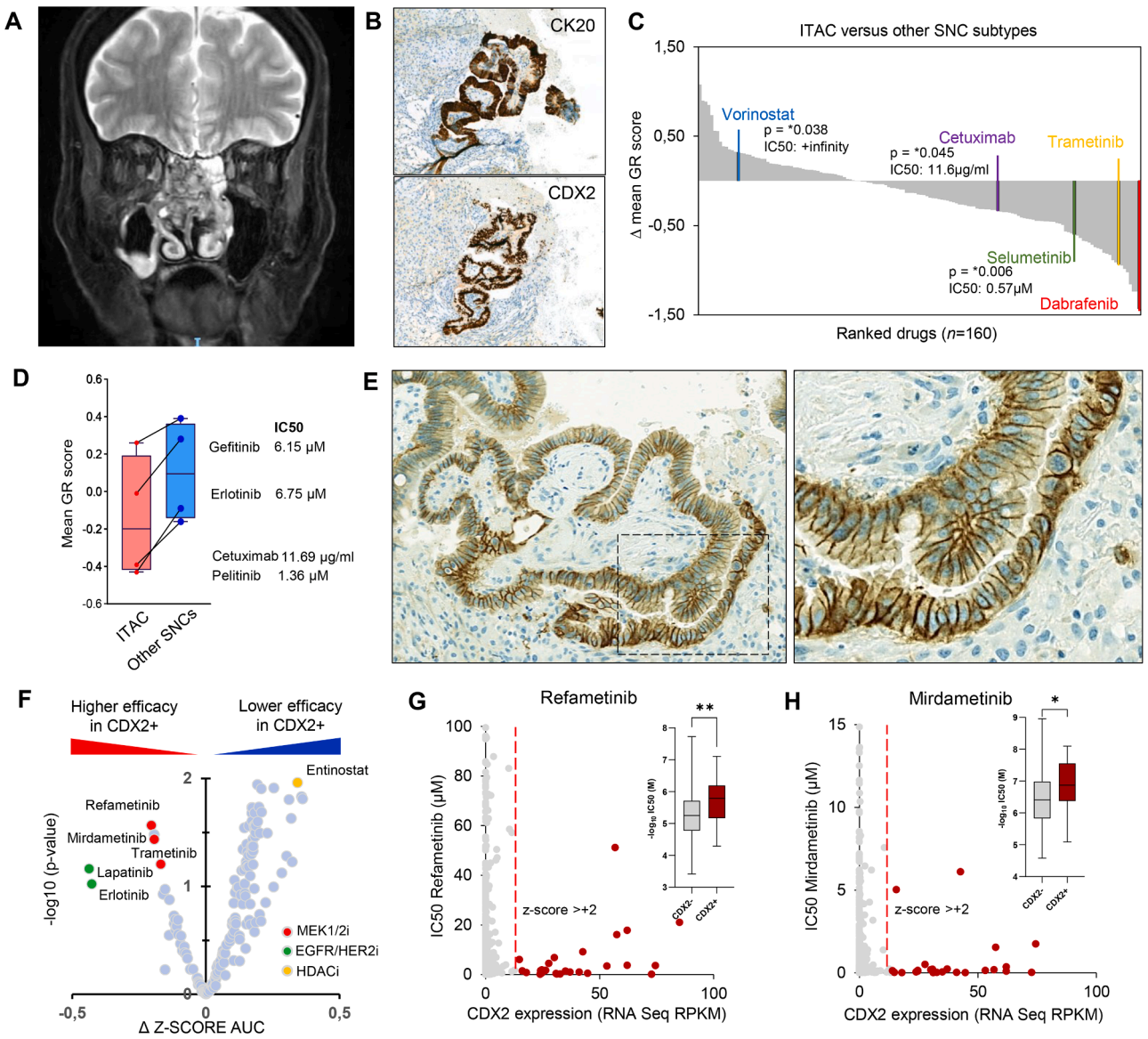

Fig. 2. **(A)** MRI image of the sinonasal intestinal-type adenocarcinoma (ITAC) patient. **(B)** Cytokeratin 20 (CK20) and CDX2 immunohistochemical (IHC) stains for differential diagnosis of ITAC. **(C)** *Ex vivo* drug screens of 160 drug molecules, assessing differences in the mean growth rate (GR) score values between patient-derived ITAC cells and other sinonasal cancer (SNC) subtypes. The selected examples of the most and least effective drugs are shown, along with the IC50 values and corresponding p-values. **(D)** Box plot showing the differences in GR scores of gefitinib, erlotinib, cetuximab, and pelitinib between ITAC cells and other SNC subtypes. **(E)** Positive EGFR IHC stain confirming overexpression of EGFR in ITAC tissue **(F)** Volcano plot showing the efficacies of selected MEK1/2-inhibitors, EGFR/HER2-inhibitors, and histone deacetylase (HDAC) inhibitors in CDX2 positive cell lines in Cancer Cell Line Encyclopedia. **(G)** and ***(H)*** Scatter plots showing CDX2 RNA expression versus IC50 values of refametinib and mirdametinib in the cell lines in Cancer Cell Line Encyclopedia and box plots showing higher efficacy of refametinib and mirdametinib in CDX2 positive than in CDX2 negative cell lines in Cancer Cell Line Encyclopedia.

neuroendocrinal cell lines compared to non-neuroendocrinal cell lines (Fig. 3E-F). These results are perfectly in line with recent data suggesting that small cell neuroendocrine phenotype is a pan-cancer type that shares therapeutic susceptibilities with hematological malignancies and that this could be harnessed for the development of treatment options beyond tissue-specific targeted therapies of neuroendocrine tumors [36].

Drug sensitivity in SNUC and SDSC

Poorly differentiated carcinomas are particularly aggressive malignancies of the sinonasal tract. SNUC is a rare and aggressive carcinoma occurring mainly in the Schneiderian mucosa of the nasal cavity. The prognosis of SNUC patients is poor [37]. Proliferation of undifferentiated cells is the characteristic feature of this carcinoma seen in histology and IHC for the stemness marker CD133 [38]. For pathologists, SNUC is a diagnosis of exclusion of differentiated types of sinonasal carcinomas. SNUCs may express CK8 (100 %) and CK7 (50 %) [39], and they often express c-KIT (CD117, 80 %), although it is not caused by activating mutations or gene amplifications [40]. Over 80 % of SNUCs harbor *IDH2* or *IDH1* mutations [41]. The SNUC patient included in the study was a 54-year-old male with a long history of smoking and a large sinonasal tumor in the superior nasal cavity extending to both orbits, in particular to the right side where tumor infiltration of the motor muscles of the eye was discovered (Fig. 4A). Histopathological examination reported overexpression of CD117 and a normal expression of INI-1, and the tumor was diagnosed as SNUC (Fig. 4B). Due to the spread of the tumor, surgical treatment was extensive including evacuation of right orbital content.

SWI/SNF complex deficient carcinomas are a recently identified,

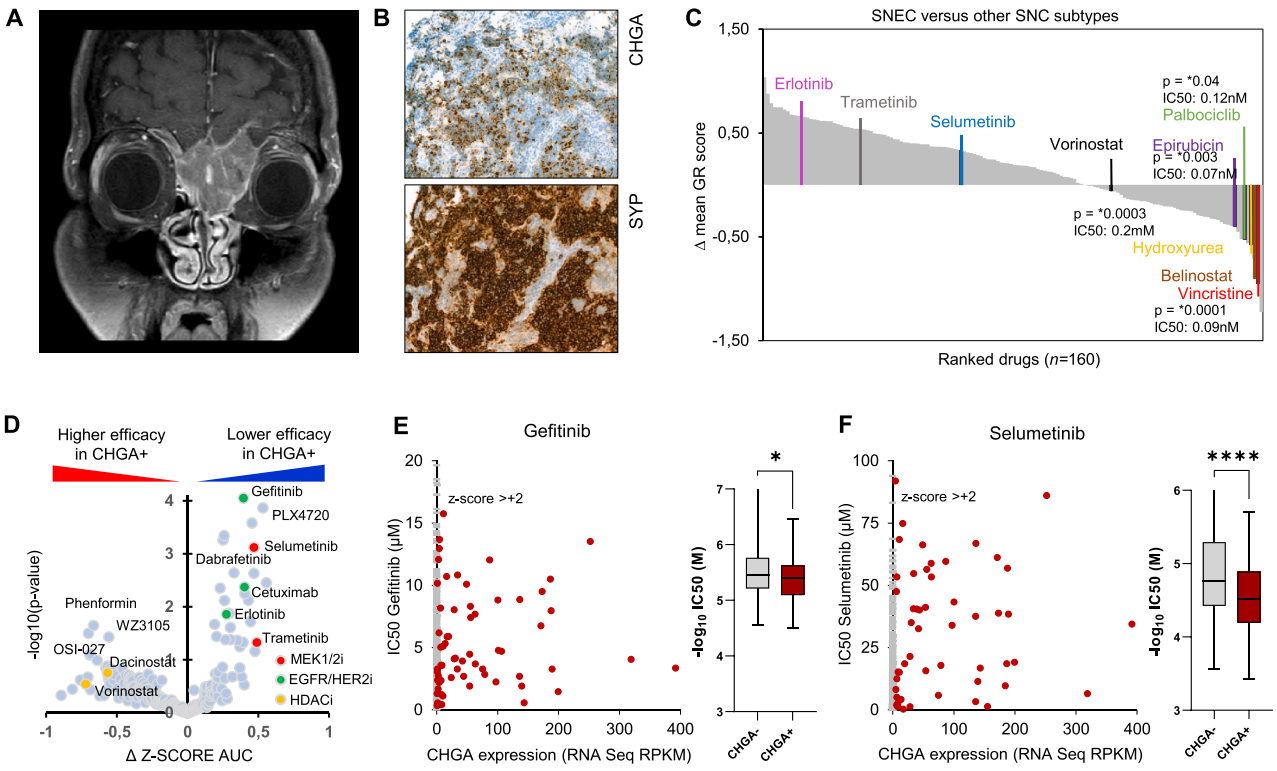

Fig. 3. **(A)** MRI image of the sinonasal neuroendocrine carcinoma (SNEC) patient. **(B)** Chromogranin A (CHGA) and synaptophysin (SYP) immunohistochemical stains for differential diagnosis of SNEC. **(C)** Ex vivo drug screens of 160 drug molecules, assessing differences in the mean growth rate (GR) score values between patient-derived SNEC cells and other sinonasal cancer (SNC) subtypes. The selected examples of the most and least effective drugs are shown, along with the IC50 values and corresponding p-values. **(D)** Volcano plot showing the efficacies of selected MEK1/2-inhibitors, EGFR/HER2-inhibitors, and histone deacetylase (HDAC) inhibitors in CHGA positive cell lines in Cancer Cell Line Encyclopedia. **(E)** and **(F)** Scatter plots showing CHGA RNA expression versus IC50 values of gefitinib and selumetinib in the cell lines in Cancer Cell Line Encyclopedia and box plots showing lower efficacy of gefitinib and selumetinib in CHGA positive than CHGA negative cell lines in Cancer Cell Line Encyclopedia.

highly aggressive group of SNCs that has been separated from SNUC [42]. These tumors comprise five subtypes including the SMARCB1 (INI-1) deficient subtype (SDSC) that displays a complete loss of the tumor suppressor encoded by *SMARCB1* gene, as indicated by negative IHC staining for INI-1 [43,44]. The SDSC patient was a 40-year-old male with a large sinonasal tumor destroying the left orbital medial wall and growing into orbital muscles and fat. In addition, the anterior part of the skull base was widely destructed, and the tumor grew into the intracranial space (Fig. 4C). In histopathological examination, the tumor was diagnosed as an undifferentiated sinonasal carcinoma with negative INI-1 expression confirming its diagnosis as SDSC (Fig. 4D). The patient was treated with extensive surgical resection, including evacuation of the left orbit, skull base resection and removal of the intracranial tumor. In comparison of the drug response profiles, SNUC and SDCS exhibited a similar drug sensitivity profile (Fig. 4E-F). Drugs targeting DNA repair mechanisms were selectively and significantly more effective in both samples compared to the other SNC subtypes (Fig. 4E-F). Of these drugs, nutlin 3A which inhibits p53/MDM2 interaction, PARP inhibitor olaparib, and EZH2 inhibitor GSK503 were selectively the most effective drugs targeting SDSC cells. The NGS analysis of the SDSC sample identified intron variants of unknown significance in genes related to signalling pathways required for response to DNA damage, including *ATM* and *ABL1* and five stop-gained mutations in the *PMS1* gene but no *SMARCB1* inactivating mutations. However, it is possible that the loss of expression may also result from intragenic copy number deletions or epigenetic mechanisms (not detected with the used NGS service). IHC examination of p53 indicated wild type pattern of p53 expression consistent with the SDSC cells being sensitive to the p53/MDM2 inhibitor RITA (Fig. 4F). In the SNUC sample, NGS indicated a rare somatic frameshift variant p.A203fs in *SMARCA4* gene. Also, variants of unknown significance in the intron area of many genes involved in the regulation of transcription or DNA repair were identified including *KMT2A, KMT2C, MLH1, MSH2* and *TP63*. In the drug screen, ATR inhibitor AZD6738, and BET inhibitor ODM-207 had the most selective cytotoxic effect on SNUC cells (Fig. 4E).

Discussion

SNCs represent a rare and diverse group of head and neck tumors with a poor prognosis. Despite the notable heterogeneity of these tumor subtypes, in many countries including Finland all SNCs are treated uniformly with surgery, radiation therapy and adjuvant chemotherapy with cisplatin. There are currently no targeted treatment strategies that consider the molecular differences between the subtypes of SNC, despite increasing evidence for potentially actionable genetic aberrations driving the different tumors. Also, the low prevalence of these tumors limits possibilities to investigate the biological differences between them. In this study, we evaluated functionally the drug sensitivity profiles of tumor cells isolated from four SNC subtypes ITAC, SNEC, SNUC and SDSC, representing biologically very different tumor types. The results were compared with histopathological and molecular pathological findings to establish functional links between the molecular characteristics of the different SNC subtypes and the associated drug sensitivities. By comparing the different subtypes, sinonasal ITAC was found to closely resemble intestinal cancers. Inhibitors targeting the EGFR/MAPK and PI3K/mTOR signaling pathways displayed significant therapeutic efficacy on the sinonasal ITAC cells aligning well with earlier reports indicating that EGFR overexpression is observed in 20–30

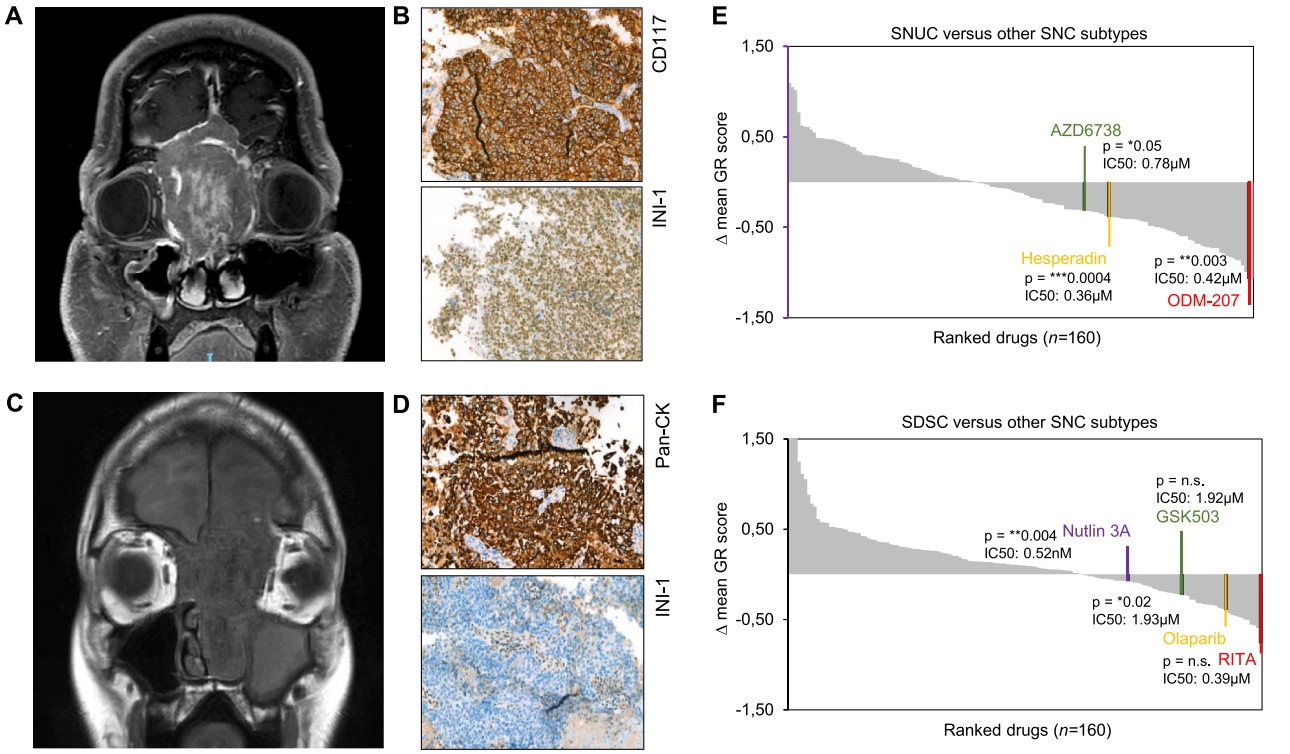

Fig. 4. **(A)** and **(C)** MRI images of the sinonasal undifferentiated carcinoma (SNUC) patient and SMARCB1 deficient sinonasal carcinoma (SDSC) patient, respectively. **(B)** and **(D)** CD117 and INI-1 immunohistochemical stains for differential diagnosis of SNUC and Pan-cytokeratin (Pan-CK) and INI-1 immunohistochemical stains for differential diagnosis of SDSC, respectively. **(E)** and **(F)** Ex vivo drug screens of 160 drug molecules, assessing differences in the mean growth rate (GR) score values between patient-derived SNEC and SDSC cells and other sinonasal cancer (SNC) subtypes. The selected examples of the most effective drugs in both subtypes are shown, along with the IC50 values and corresponding p-values.

% of sinonasal ITACs, while *KRAS* mutations are absent [25,45,46]. In the present case, EGFR overexpression was confirmed by IHC staining and no *KRAS* mutations were observed explaining the significant sensitivity to EGFR-TKI in this case. Since sinonasal ITAC is often a well-differentiated adenocarcinoma, and activating mutations in the downstream genes of the EGFR cascade are rare, sinonasal ITACs are potential candidates for anti-EGFR therapies and e.g., selumetinib [47] with CDX2 serving as a potential prognostic marker [48].

The SNEC cells were found to share therapeutic susceptibility with hematological cancers. The *ex vivo* drug screening revealed apparent differences in drug sensitivity/resistance profiles between sinonasal neuroendocrine tumor cells and the other SNC subtypes. SNEC tumors are poorly differentiated, and the cell division and growth regulation do not occur through epithelial cell differentiation dependent signalling pathways such as EGFR/HER2, but is controlled rather by the upregulation of stem cell-like signalling pathways [49,50]. Accordingly, SNEC cells were non-responsive to drugs targeting EGFR/MAPK signalling pathways. Instead, drugs inhibiting cell division such as DNA alkylating agents, topoisomerase inhibitors and tubulin poisons, and epigenetic mechanisms such as HDAC inhibitors displayed higher efficacy on SNEC cells. Similar results on the differential drug sensitivity/resistance of neuroendocrine tumor cells has also been demonstrated in earlier large-scale data sets where cancer cells with neuroendocrine differentiation have been shown to share drug sensitivity profiles with hematological cancers [26,36].

SNUC and SDSC cells were found to be vulnerable to DNA repair targeted therapies. In addition to SNUC and SDSC being histopathologically reminiscent tumors, the drug sensitivity and resistance profiles of tumor cells derived from these tumors were also found to resemble each other. Both subtypes were significantly more sensitive to drugs that inhibit DNA repair mechanisms than the other SNC subtypes. A rare *SMARCA4* somatic frameshift variant p. A203fs was identified in the SNUC sample cells leading probably to an unfunctional protein and thus SMARCA4-deficiency. It has been proposed that SMARCA4-deficient sinonasal carcinomas could be a genetically distinct aggressive entity of SMARCB1-intact undifferentiated sinonasal malignancies [51]. SMARCA4 and INI-1 (encoded by *SMARCB1*) are both parts of the same SWItch/Sucrose Non-Fermentable (SWI/SNF) complex which functions in chromatin remodeling and is associated with many cellular functions such as repair of damaged DNA and cell growth [52,53]. The drug screens identified several selectively effective drugs in SNUC and SDSC cells that have been reported to induce synthetic lethal interactions in SWI/SNF – deficient cancers [54]. These include Aurora A kinase inhibitor hesperidin, ATR inhibitor AZD6738 and BET inhibitor ODM-207 in SNUC, and MDM2/4 inhibitor nutlin 3A, PARP inhibitor olaparib and EZH2 inhibitor GSK503 in SDSC. Loss of INI1 expression leads to oncogenic activation of a transcriptional repressor EZH2, a catalytic subunit of Polycomb repressive complex 2 [55,56]. Targeting the oncogenic dependency of INI-1/*SMARCB1*-deficient tumors on EZH2 has been studied and shown to be a potential treatment option in patients with loss of INI-1 [57] and the strategy could thus also be functional for INI-1/*SMARCB1*-deficient sinonasal cancers.

Conclusion

In this study, we utilized patient-derived sinonasal cancer cells as models to functionally study molecular and histological subtype selective therapeutic opportunities in different sinonasal cancers. To date, this is the first reported study that has utilized primary patient derived cells to assess general drug sensitivity in individual sinonasal tumors. As

the incidence rate of newly diagnosed SNCs is low, e.g., ~0.15 % of all newly diagnosed cancers in Finland (5-year average, 2017–21), the present study is limited by the fact that only four patients could be recruited through our center. However, our study, combined with the discussed previous reports on the diversity of SNC subtypes, emphasize the urgent need for a general review of the treatment approaches for patients affected with the different subtypes of sinonasal cancers. The remarkable biological differences and the various targetable genomic aberrations of individual sinonasal tumors should be considered and used to motivate the development of alternative targeted treatments. We believe that our work can pave the way for repurposing several existing drugs for treatment of SNCs. This is based on our findings that these tumors carry same actionable genetic aberrations as some other cancers for which these drugs are already approved. In summary, our results demonstrate that patient-derived sinonasal cancer cells are relevant models that can be used to identify targeted treatments for SNC patients. To extend findings of this study and to increase the diversity of SNC patient samples included for similar analyses, collaborative research efforts will be essential. We therefore aim to apply this workflow in future collaborative studies of additional sinonasal cancer patients, in the hope of identifying additional treatment options for at least some of them and to further enhance our understanding and management of these rare and challenging malignancies.

CRediT authorship contribution statement

Noora Lehtinen: Writing – review & editing, Writing – original draft, Visualization, Investigation, Formal analysis, Data curation, Conceptualization. **Janne Suhonen:** Formal analysis, Data curation. **Kiesha Rice:** Writing – original draft, Investigation. **Eetu Välimäki:** Methodology, Investigation, Formal analysis. **Mervi Toriseva:** Visualization, Resources, Investigation. **Johannes Routila:** Writing – review & editing, Resources. **Perttu Halme:** Writing – original draft, Resources. **Melissa Rahi:** Resources, Investigation. **Heikki Irjala:** Writing – review & editing, Writing – original draft, Supervision, Resources, Investigation. **Ilmo Leivo:** Writing – review & editing, Writing – original draft, Resources, Investigation. **Markku Kallajoki:** Writing – review & editing, Writing – original draft, Supervision, Resources, Investigation. **Matthias Nees:** Resources, Funding acquisition. **Teijo Kuopio:** Writing – review & editing, Writing – original draft, Supervision, Investigation. **Sami Ventelä:** Writing – review & editing, Writing – original draft, Resources, Investigation. **Juha K. Rantala:** .

Declaration of competing interest

The authors declare the following financial interests/personal relationships which may be considered as potential competing interests:

Juha K. Rantala is the founder of Misvik Biology Oy, and Noora Lehtinen, Janne Suhonen, Kiesha Rice and Eetu Välimäki are employees of Misvik Biology Oy.

Supplementary materials

Supplementary material associated with this article can be found, in the online version, at doi:10.1016/j.tranon.2024.101935.

References

[1] J.H. Turner, D.D. Reh, Incidence and survival in patients with sinonasal cancer: a historical analysis of population-based data, Head Neck 34 (2012) 877–885.

[2] B. Ansa, M. Goodman, K. Ward, et al., Paranasal sinus squamous cell carcinoma incidence and survival based on surveillance, epidemiology, and end results data, 1973 to 2009, Cancer 119 (2013) 2602–2610.

[3] D.R. Youlden, S.M. Cramb, S. Peters, et al., International comparisons of the incidence and mortality of sinonasal cancer, Cancer Epidemiol. 37 (2013) 770–779.

[4] S. Sanghvi, M.N. Khan, N.R. Patel, S. Yeldandi, S. Baredes, J.A. Eloy, Epidemiology of sinonasal squamous cell carcinoma: a comprehensive analysis of 4994 patients, Laryngoscope 124 (2014) 76–83.

[5] Organisation mondiale de la santé, Lyon: international agency for research on cancer. Centre International De Recherche Sur Le cancer, Eds. WHO Classification of Head and Neck Tumours, 4th ed., World health organization classification of tumours, 2017.

[6] A. Weaver, J.J. Loh, H. Vandenberg, et al., Combined modality therapy for advanced head and neck cancer, Am. J. Surg. 140 (1980) 549–552.

[7] M.R. Gore, Survival in sinonasal and middle ear malignancies: a population-based study using the SEER 1973–2015 database, BMC Ear Nose Throat Disord. 18 (2018) 13.

[8] F. López, C. García Inclán, J. Pérez-Escuredo, et al., KRAS and BRAF mutations in sinonasal cancer, Oral Oncol. 48 (2012) 692–697.

[9] A. Franchi, D.R.D. Innocenti, A. Palomba, et al., Low prevalence of K-RAS, EGF-R and BRAF mutations in sinonasal adenocarcinomas. Implications for anti-EGFR treatments, Pathol. Oncol. Res. 20 (2014) 571–579.

[10] C. Riobello, A. López-Hernández, V.N. Cabal, et al., IDH2 Mutation Analysis in Undifferentiated and Poorly Differentiated Sinonasal Carcinomas for Diagnosis and Clinical Management, Am. J. Surg. Pathol. 44 (2020) 396–405.

[11] J.G. Martínez, J. Pérez-Escuredo, F. López, et al., Microsatellite instability analysis of sinonasal carcinomas, Otolaryngology–Head Neck Surg. 140 (2009) 55–60.

[12] C. Riobello, B. Vivanco, S. Reda, et al., Programmed death ligand-1 expression as immunotherapeutic target in sinonasal cancer, Head Neck 40 (2018) 818–827.

[13] H. Quan, L. Yan, S. Wang, S. Wang, Clinical relevance and significance of programmed death-ligand 1 expression, tumor-infiltrating lymphocytes, and p16 status in sinonasal squamous cell carcinoma, Cancer Manag. Res. 11 (2019) 4335–4345.

[14] N. Nykänen, R. Mäkelä, A. Arjonen, et al., Ex vivo drug screening informed targeted therapy for metastatic parotid squamous cell carcinoma, Front. Oncol. 11 (2021) [Internet][cited 25 January 2023]Available at: https://www.frontiersin.org/articles/10.3389/fonc.2021.735820.

[15] R. Mäkelä, A. Arjonen, A. Suryo Rahmanto, et al., Ex vivo assessment of targeted therapies in a rare metastatic epithelial–myoepithelial carcinoma, Neoplasia 22 (2020) 390–398.

[16] R. Mäkelä, A. Arjonen, V. Härmä, et al., Ex vivo modelling of drug efficacy in a rare metastatic urachal carcinoma, BMC Cancer 20 (2020) 590.

[17] INVIEW Oncoprofiling (591 genes) (former INVIEW Oncopanel All-in-one) [Internet]. [cited 27 January 2023]. Available at: https://eurofinsgenomics.eu/en/next-generation-sequencing/applications/oncology-solutions/inview-oncoprofiling/.

[18] J. Routila, I. Leivo, H. Minn, J. Westermarck, S. Ventelä, Evaluation of prognostic biomarkers in a population-validated Finnish HNSCC patient cohort, Eur. Arch. Otorhinolaryngol. 278 (2021) 4575–4585.

[19] M. Hafner, M. Niepel, M. Chung, P.K Sorger, Growth rate inhibition metrics correct for confounders in measuring sensitivity to cancer drugs, Nat. Methods 13 (2016) 521–527.

[20] M. Ghandi, F.W. Huang, J. Jané-Valbuena, et al., Next-generation characterization of the cancer cell line encyclopedia, Nature 569 (2019) 503–508.

[21] M.T. Kennedy, R.C.K. Jordan, K.W. Berean, B. Perez-Ordoñez, Expression pattern of CK7, CK20, CDX-2, and villin in intestinal-type sinonasal adenocarcinoma, J. Clin. Pathol. 57 (2004) 932–937.

[22] A. Franchi, D. Massi, A. Palomba, M. Biancalani, M. Santucci, CDX-2, cytokeratin 7 and cytokeratin 20 immunohistochemical expression in the differential diagnosis of primary adenocarcinomas of the sinonasal tract, Virchows Arch. 445 (2004) 63–67.

[23] H.P. Cathro, S.E. Mills, Immunophenotypic differences between intestinal-type and low-grade papillary sinonasal adenocarcinomas: an immunohistochemical study of 22 cases utilizing CDX2 and MUC2, Am. J. Surg. Pathol. 28 (2004) 1026–1032.

[24] B. Perez-Ordonez, N.N. Huynh, K.W. Berean, R.C.K. Jordan, Expression of mismatch repair proteins, beta catenin, and E cadherin in intestinal-type sinonasal adenocarcinoma, J. Clin. Pathol. 57 (2004) 1080–1083.

[25] F. Projetti, K. Durand, A. Chaunavel, et al., Epidermal growth factor receptor expression and KRAS and BRAF mutations: study of 39 sinonasal intestinal-type adenocarcinomas, Hum. Pathol. 44 (2013) 2116–2125.

[26] F. Iorio, T.A. Knijnenburg, D.J. Vis, et al., A landscape of pharmacogenomic interactions in cancer, Cell. 166 (2016) 740–754.

[27] P. Sánchez-Fernández, C. Riobello, M. Costales, et al., Next-generation sequencing for identification of actionable gene mutations in intestinal-type sinonasal adenocarcinoma, Sci. Rep. 11 (2021) 2247.

[28] T.T. Wu, L. Barnes, A. Bakker, P.A. Swalsky, S.D. Finkelstein, K-ras-2 and p53 genotyping of intestinal-type adenocarcinoma of the nasal cavity and paranasal sinuses, Mod. Pathol. 9 (1996) 199–204.

[29] R. Holmila, J. Bornholdt, P. Heikkilä, et al., Mutations in TP53 tumor suppressor gene in wood dust-related sinonasal cancer, Int. J. Cancer 127 (2010) 578–588.

[30] J. Pérez-Escuredo, J.G. Martínez, B. Vivanco, et al., Wood dust-related mutational profile of TP53 in intestinal-type sinonasal adenocarcinoma, Hum. Pathol. 43 (2012) 1894–1901.

[31] Robert W. Werling, Hadi Yaziji, Carlos E. Bacchi, Allen M Gown, CDX2, a highly sensitive and specific marker of adenocarcinomas of intestinal origin. An immunohistochemical survey of 476 primary and metastatic carcinomas, Am. J. Surg. Pathol. 27 (2003) 303–310.

[32] H. Beltran, D. Prandi, J.M. Mosquera, et al., Divergent clonal evolution of castration-resistant neuroendocrine prostate cancer, Nat. Med. 22 (2016) 298–305.

[33] J. George, J.S. Lim, S.J. Jang, et al., Comprehensive genomic profiles of small cell lung cancer, Nature 524 (2015) 47–53.

[34] A. Davies, A. Zoubeidi, L.A. Selth, The epigenetic and transcriptional landscape of neuroendocrine prostate cancer, Endocr. Relat. Cancer 27 (2020) R35–R50.
[35] K. Fan, C. Zhang, Y. Qi, et al., ProgNOSTIC VALUe of EZH2 in non-small-cell lung cancers: a meta-analysis and bioinformatics analysis, Biomed. Res. Int. 2020 (2020) 2380124.
[36] N.G. Balanis, K.M. Sheu, F.N. Esedebe, et al., Pan-cancer convergence to a small-cell neuroendocrine phenotype that shares susceptibilities with hematological malignancies, Cancer Cell 36 (2019) 17–34, e7.
[37] D.A. Reiersen, M.E. Pahilan, A.K. Devaiah, Meta-analysis of treatment outcomes for sinonasal undifferentiated carcinoma, Otolaryngol. Head Neck Surg. 147 (2012) 7–14.
[38] M. Ansari, S. Guo, S. Fakhri, et al., Sinonasal undifferentiated carcinoma (SNUC): morphoproteomic-guided treatment paradigm with clinical efficacy, Ann. Clin. Lab. Sci. 43 (2013) 45–53.
[39] A. Franchi, M. Moroni, D. Massi, M. Paglierani, M. Santucci, Sinonasal undifferentiated carcinoma, nasopharyngeal-type undifferentiated carcinoma, and keratinizing and nonkeratinizing squamous cell carcinoma express different cytokeratin patterns, Am. J. Surg. Pathol. 26 (2002) 1597–1604.
[40] R.D. Chernock, A. Perry, J.D. Pfeifer, J.A. Holden, J.S Lewis Jr, Receptor tyrosine kinases in sinonasal undifferentiated carcinomas—Evaluation for EGFR, c-KIT, and HER2/neu expression, Head Neck 31 (2009) 919–927.
[41] S. Dogan, D.J. Chute, B. Xu, et al., Frequent IDH2 R172 mutations in undifferentiated and poorly-differentiated sinonasal carcinomas, J. Pathol. 242 (2017) 400–408.
[42] A. Agaimy, A. Hartmann, C.R. Antonescu, et al., SMARCB1 (INI-1)-deficient sinonasal carcinoma: a series of 39 cases expanding the morphological and clinicopathological spectrum of a recently described entity, Am. J. Surg. Pathol. 41 (2017) 458–471.
[43] A. Agaimy, M. Koch, M. Lell, et al., SMARCB1(INI1)-deficient sinonasal basaloid carcinoma, Am. J. Surg. Pathol. 38 (2014) 1274–1281.
[44] J.A. Bishop, C.R. Antonescu, W.H. Westra, SMARCB1 (INI-1) deficient carcinomas of the sinonasal tract, Am. J. Surg. Pathol. 38 (2014) 1282–1289.
[45] V. Szablewski, J. Solassol, F. Poizat, et al., EGFR Expression and KRAS and BRAF Mutational Status in Intestinal-Type Sinonasal Adenocarcinoma, Int. J. Mol. Sci. 14 (2013) 5170–5181.
[46] F. Projetti, L. Mesturoux, B. Coulibaly, et al., Study of MET protein levels and MET gene copy number in 72 sinonasal intestinal-type adenocarcinomas, Head Neck 37 (2015) 1563–1568.
[47] A. Markham, S.J. Keam, Selumetinib: first approval, Drugs 80 (2020) 931–937.
[48] K. Aasebø, A. Dragomir, M. Sundström, et al., CDX2: a prognostic marker in metastatic colorectal cancer defining a better braf mutated and a worse kras mutated subgroup, Front. Oncol. 10 (2020) [Internet][cited 25 January 2023] Available at: https://www.frontiersin.org/articles/10.3389/fonc.2020.00008.
[49] T.M. Malta, A. Sokolov, A.J. Gentles, et al., Machine learning identifies stemness features associated with oncogenic dedifferentiation, Cell 173 (2018) 338–354, e15.
[50] B.A. Smith, N.G. Balanis, A. Nanjundiah, et al., A human adult stem cell signature marks aggressive variants across epithelial cancers, Cell Rep. 24 (2018) 3353–3366, e5.
[51] A. Agaimy, W. Weichert, SMARCA4-deficient sinonasal carcinoma, Head Neck Pathol. 11 (2017) 541–545.
[52] C.L. Peterson, A. Dingwall, M.P. Scott, Five SWI/SNF gene products are components of a large multisubunit complex required for transcriptional enhancement, Proc. Natl. Acad. Sci. U S A 91 (1994) 2905–2908.
[53] J. Masliah-Planchon, I. Bièche, J.-M. Guinebretière, F. Bourdeaut, O. Delattre, SWI/SNF chromatin remodeling and human malignancies, Annu. Rev. Pathol. 10 (2015) 145–171.
[54] M. Wanior, A. Krämer, S. Knapp, A.C. Joerger, Exploiting vulnerabilities of SWI/SNF chromatin remodelling complexes for cancer therapy, Oncogene 40 (2021) 3637–3654.
[55] J.A. Simon, C.A. Lange, Roles of the EZH2 histone methyltransferase in cancer epigenetics, Mutat. Res. 647 (2008) 21–29.
[56] B.G. Wilson, X. Wang, X. Shen, et al., Epigenetic antagonism between Polycomb and SWI/SNF complexes during oncogenic transformation, Cancer Cell 18 (2010) 316–328.
[57] M. Gounder, P. Schöffski, R.L. Jones, et al., Tazemetostat in advanced epithelioid sarcoma with loss of INI1/SMARCB1: an international, open-label, phase 2 basket study, The Lancet Oncol. 21 (2020) 1423–1432.